NUMERICAL SIMULATION AND EXPERIMENTAL TEST CAMPAIGN OF COMPOSITE BRAIDED FRAMES UNDER A COMBINED COMPRESSION/BENDING LOAD

M. Vinot[1], P. Schatrow[1], R. Sturm[2], F. Heieck[3] and D. Fernández[3]

[1]German Aerospace Center (DLR), Institute of Structures and Design, 70569 Stuttgart, Germany
Email: mathieu.vinot@dlr.de, Web Page: www.dlr.de/bt/en/
[2]German Aerospace Center, Institute of Vehicle Concepts, 70569 Stuttgart, Germany
[3]University of Stuttgart, Institute of Aircraft Design, 70569 Stuttgart, Germany

Keywords: braided composites, combined compression/bending load, energy absorption, numerical simulation, test campaign

Abstract

This paper discusses manufacturing process, experimental testing and numerical simulation of braided Ω-frame segments bonded to a multiaxial fabric skin which represent the typical airframe structure. The Ω-frame preforms were manufactured using the circular braiding process and impregnated with resin by Vacuum Asissted Process (VAP) technique. The experimental testing was conducted quasistatically on a test setup which introduces simultaneous compression and bending loads in the specimen segment. The experimental results of the test campaing were used to develop numerical methods for the design of braided structures. The simulations were performed using explicit FE code LS-DYNA.
Different fibre architectures were investigated with the aim of increasing energy absorption of Ω-frames subjected to simultaneous compression and bending mode which typically occures in an aircraft crash. A further priority of this study was the development of a trigger mechanism for the Ω-frame which is required to initiate frame failure at defined location and load.

1. Introduction

Energy absorption potential is a significant parameter for the sizing of crash-relevant aircraft components. Conventional primary aircraft structures made of aluminium alloys offer sufficient crashworthiness by their ductile failure behaviour. On the other hand, primary aircraft structures made of composite materials may show at complex or unfavourable loading conditions brittle failure behaviour with low energy absorption. A promising approach to increase energy absorption of composite structures which are loaded at complex loading conditions (e.g. combined compression/bending load) is the circular braiding manufacturing process. Braided composites take advantage of the high interlacing and nesting of the rovings. In this context, the circular braiding manufacturing process offers the possibility to improve the absorption potential of airframe structures by modifying fibre architecture.

The project DLR@UniST, cooperation between the Institute of Aircraft Design of the University of Stuttgart and the Institute of Structures and Design of the German Aerospace Center, aims at reducing the experimental effort by use of numerical approaches for a reliable prediction of braided composite structures under realistic loading conditions. The experimental and numerical test campaign follows a "building-block" approach shown in Figure 1. On the coupon level compression and tension tests were conducted to characterise the braiding material. Following, frames segments with generic C-shaped cross section were investigated on element level subjected to pure bending mode [1]. The results from [1] showed significant influence of the energy absorption by modification of the fibre architecture (biaxial or triaxial braids, material hybridisation, braiding angle) compared to standard braided frames. Finally, on the component level typical aircraft structural components consisting of a Ω-frame segment bonded to a multiaxial fabric skin were investigated under realistic loading conditions. One focus of

Excerpt from ISBN 978-3-00-053387-7

the present study was the transfer of the most promising fibre architectures from [1] on the more complex component level of the building block approach. On the element level the selected fibre architectures showed significant increase of energy absorption whereas on the component level no significant energy absorption was observed compared to the standard braided frames. A second priority of this study was the development of a trigger mechanism for the Ω-frame which is required to initiate frame failure at defined location and load.

Prior to experimental testing the investigated specimen segments were scanned with the computer tomography technique in order to detect possible manufacturing perturbations that could influence the test results.

At each stage of the campaign, numerical models based on the homogenization of braid properties on shell elements have been developed and implemented in the finite-element software LS-DYNA. The global behaviour of the Ω-frame has been successfully predicted for the investigated braid architectures.

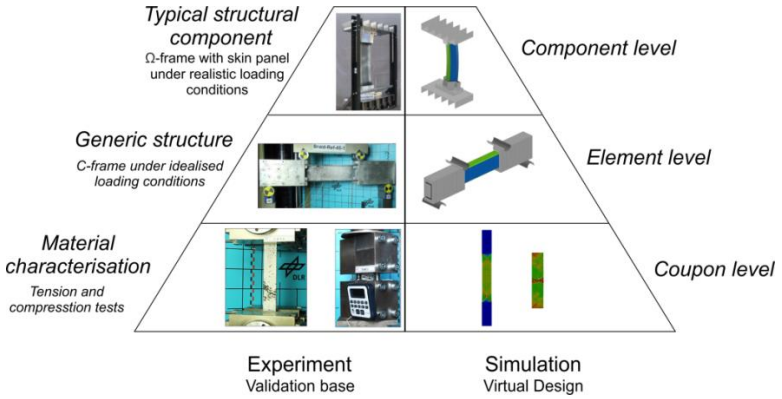

Figure 1. Experimental test-pyramid in DLR@UniST, following the "building-block" approach

2. Manufacturing

2.1. Preform manufacturing using circular braiding process

The Ω-frame segments were manufactured using the circular braiding process. It allows for the production of geometrically complex components with a large range of possibilities to optimize the fibre architecture and to combine different types of yarn materials.

In this work, a radial braiding machine RF 1-176-100 by the company Herzog Maschinenbau GmbH & Co. is used in combination with an industrial robot (Figure 2), which guides the braid mandrel through the center of the machine with a defined velocity. By adjusting the velocity, the braid angle – which is defined as the angle between the braid fibres and the product axis – can be determined in a range of approximately ±30° to ±70°, depending on the mandrel geometry and the fibre setup. Additionally, axial yarns can be introduced along the product axis, which are fed in from the outer section of the braiding machine. Braids with these zero degree yarns are called triaxial braids, while biaxial braids consist of braiding yarns only, which are aligned diagonally to the product axis.

Several Ω-frames designs with different fibre architectures were manufactured and tested. Two different carbon fibre Ω-frames designs are shown Table 1: A braided reference frame with ±45° braid angle and a frame with a trigger at the inner flange of the frame. The trigger was manufactured during the braiding process by overbraiding of a displacer with a diameter of 10 mm which was attached on the mandrel (Figure 3). The displacer deflects the fibres around the circular pin and creates a hole representing a weak spot in the frame. It is thus possible to initiate the failure of the frame at a

Excerpt from ISBN 978-3-00-053387-7

predetermined location, which is crucial for controlling the energy absorption of frames under bending load.

For all specimens, TohoTenax® HTS40 F13 12K carbon fibres are used. Four layers of braid are used for the frames, each consisting of two ±45° yarn systems and additional axial yarns distributed along the inner flange of the specimens, where high bending and compression loads occur during testing.

Figure 2. Radial braiding machine at IFB

Figure 3. Overbraided mandrel with tapered displacement element

Table 1. Overview of manufactured Ω-frame specimens.

Specimen no.	Description	Braid angle	Braid setup	Layup
1	Reference carbon braided frame	±45°	Biaxial carbon braid in the web, triaxial carbon braid in inner flange	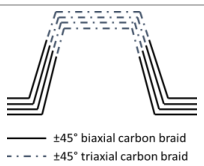
2	Carbon frame with trigger	±45°	Biaxial carbon braid in the web, triaxial carbon braid in inner flange	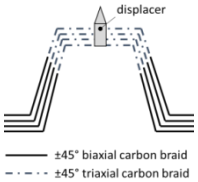

2.2. Resin infusion

The resulting braided preform was impregnated using Vacuum Asissted Process (VAP) technique, which is a VARI-based process (Vacuum Assisted Resin Infusion) that uses an additional semi-permeable membrane to create a double-chamber bagging setup. This membrane allows gasses to flow through it, but it is impermeable to liquids. Figure 4 shows the VAP configuration, where the resin inlet and the bleeding line are separated by the semi-permeable membrane. As in a VARI infusion, vacuum is still used to draw the resin through the preform, but in this case the semi-permeable membrane will contain the resin within chamber 2.

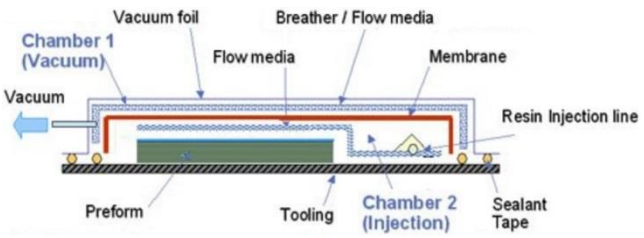

Figure 4. VAP infusion setup

Figure 5. VAP infusion setup for 2 Ω-frames

Excerpt from ISBN 978-3-00-053387-7

This setup makes the infusion of thicker, less permeable preforms possible and ensures a full impregnation, especially in parts with complex 3D-geometries like the one considered in this study. Figure 5 shows the actual setup used to infuse two Ω-frames at the same time. The multi-purpose tooling designed for this study is shown on the left of Figure 6. Once the braiding process is finished, it can be converted into its infusion form. The closed braided preform is cut open so that the flanges can be folded out to form the Ω-shaped cross section. On the right of Figure 6 it is shown how the ureol braiding attachments are removed and the aluminium tooling core is placed on the curved infusion plate.

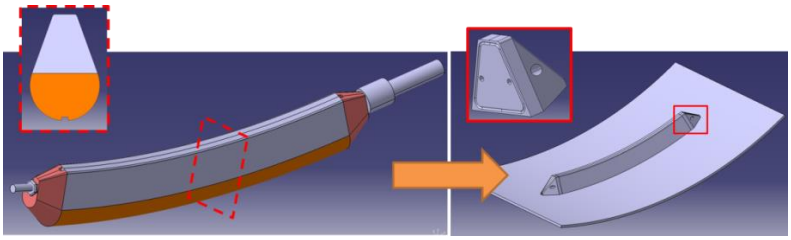

Figure 6. Multi-purpose tooling in (left) braiding mode and (right) infusion mode

Additional aluminium cones are attached on either side of the aluminium core in order to obtain a smooth transition for the vacuum bag. The chosen resin system was Hexcel's HexFlow® RTM6, a mono-component epoxy that has been certified for aerospace applications. In order to carry out an injection, RTM6 has to be heated up to 80 °C to achieve an appropriate viscosity and injection tooling has to be at 120 °C to ensure full impregnation. After infusion, the Ω-frame specimens are cut with a wet saw to the required dimensions. Skin panels are manufactured out of Prepreg with a stacking sequence of $[+45,90,-45,+45,-45,0,+45,-45,90_{1/2}]_s$ and cut separately. Frames and skin (Figure 7) are bonded with the aircraft certified film adhesive Cytec FM® 300K under vacuum pressure.

Figure 7. Impregnated Ω-frame with bonded multiaxial fabric skin

3. Experimental testing

3.1. Test setup

In the past, several drop test of typical metallic fuselage sections were conducted to create a database for crashworthiness standards of future transport aircraft and to increase passenger survival rate [2], [3]. One typical crash kinematics observed from these drop tests is shown in Figure 8a. In this kinematics the frame failure occurs first at the impact point and second between 40°-60° in circumferential direction starting from the impact point which results in an unrolling of the lower fuselage shell. The developing frame hinge at the impact point rotates in an opening direction and the frame hinges above the cargo crossbeam in a closing direction. In the present study the frame failure with a closing hinge above the cargo crossbeam was studied. At the location of the closing hinge the frame fails as a result of the bending moment around the fuselage section longitudinal axis and the compressive force normal to the frame cross section.

In [4], [5] a test setup was designed for testing of structural components in case of simultaneously occurring bending moment and normal force. Figure 8b illustrates the schematic drawing of the test setup with a specimen in a closing configuration. The specimen is clamped between two plates with a pinned support type. Additionally, the upper plate is designed to move along a guidance system to

Excerpt from ISBN 978-3-00-053387-7

apply an off-centre load on the specimen. The ratio between the bending moment and the normal force acting on the specimen cross section corresponds to the distance between the location of the closing hinge which develops after frame failure and the off-centre force along the guidance system. The magnitude of this value was estimated from numerical simulation to be about 200 mm [4].

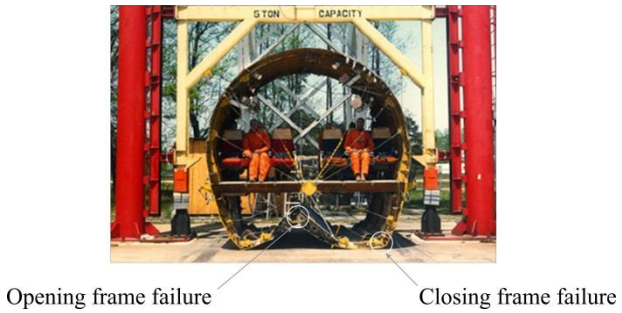

a) Typical crash kinematics [6]

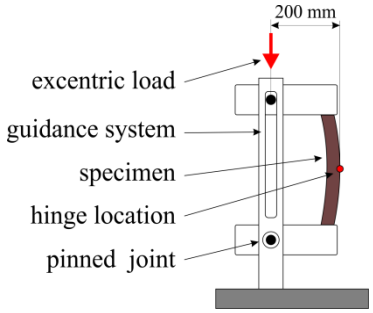

b) Schematic drawing of the test setup [4]

Figure 8. Development of the test setup

The Ω-frame segments with the multiaxial skin were embedded in aluminium clampings for load introduction (Figure 9a). The gaps between the aluminium clampings and the Ω-frame segment were filled with an epoxy resin LR-285 and its curing agent LH-285 in the specified ratio. The compressive stiffness of the resin system was increased by addition of milled carbon fibres. Figure 9b shows the Ω-frame segment embedded in aluminium clampings and equipped with strain gauges. Figure 9c illustrates the prepared Ω-frame segment in the test setup.

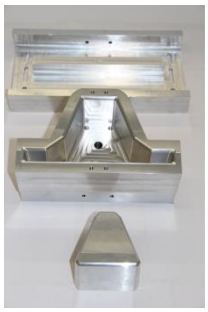

a) Aluminium clamping

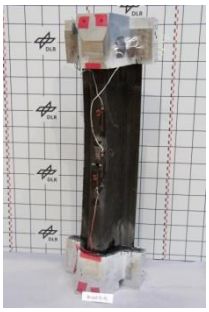

b) Ω-frame segment embedded in aluminium clampings

c) Ω-frame segment in test setup

Figure 9. Test preparation of the Ω-frame segment

The quasi-static tests were performed on a Zwick Roell 1475 universal testing machine with a constant crosshead velocity of v = 2 mm/min up to failure initiation and v = 10 mm/min in post failure phase. The maximum crosshead displacement was about s = 100 mm.

3.2. Test results

This paragraph discusses test results for the Ω-frame with the trigger which was investigated to initiate frame failure at a defined location and load. The weakening of the inner frame was sufficient to reduce the failure load of the untriggered Ω-frame segment from 37.5 kN [7] to 28.5 kN and the failure displacement from 15.1 mm [7] to 11.4 mm. The stiffness of the Ω-frame segment was almost not influenced by the trigger. Figure 10 depicts the test sequence of the Ω-frame segment from the front and the side view. Force displacement curves of the experiment and the simulation are compared in chapter 4.

Excerpt from ISBN 978-3-00-053387-7

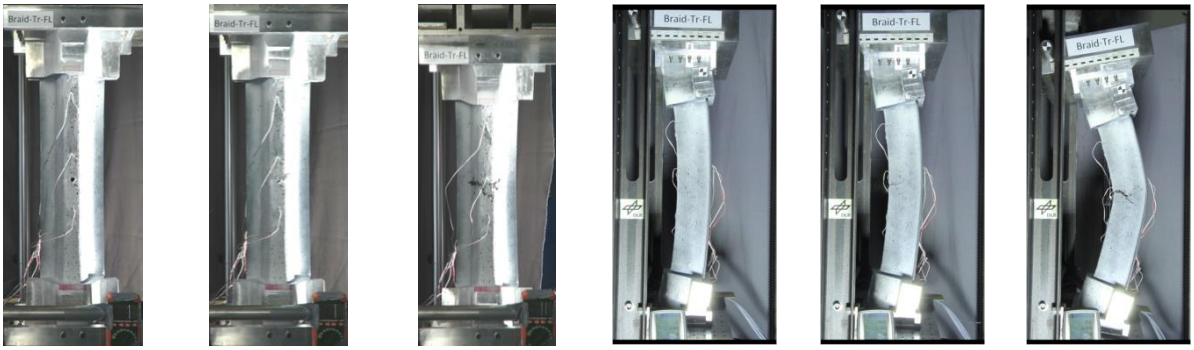

a) s = 0 mm b) s ≈ 11.4 mm c) s ≈ 80 mm d) s = 0 mm e) s ≈ 11.4 mm f) s ≈ 80 mm

Figure 10. Test sequence for a Ω-frame design with trigger

The frame failure is initiated in the inner flange by the trigger. Starting from the inner flange the crack propagates through the web up to the frame foot as shown in Figure 11. In the area of triaxial braid the crack is developing perpendicular to zero degree yarns. Having reached the biaxial braid, the crack is developing along the bias yarns at an angle of approximately 45° which corresponds to the braiding angle.

Figure 11. Crack propagation in the web of Ω-frame segment

4. Virtual testing

4.1. Geometry and model on the structure scale

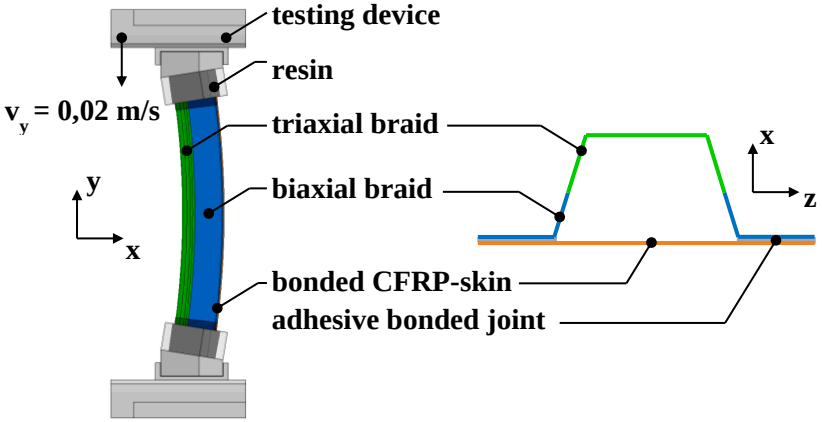

Figure 12. FE-Model of the Ω-frame and test setup

The test specimen and the whole test setup were modelled to recreate the experimental test conditions as closely as possible as illustrated in Figure 12. The loading velocity is applied on the upper steel plate and has been increased to 0.02 m/s to reduce the computing time while avoiding strain rate effects. The boundary condition of the upper plate with free rotation above the z-direction and translational displacement along the y-direction were modelled by constraining the translational

Excerpt from ISBN 978-3-00-053387-7

degrees of freedom in x and z-directions ($u_x = u_z = 0$) and rotational degrees of freedom above x- and y-directions ($\phi_x = \phi_y = 0$). The boundary condition of the lower plate were modelled by constraining all but the rotational degree of freedom above z-direction ($u_x = u_y = u_z = 0$; $\phi_x = \phi_y = 0$). The adhesive bonded joint between the Ω-frame and skin panel is simplified using the tiebreak contact in LS-DYNA. This contact type is based on the cohesive zone theory and allows for the simulation of crack propagation in the bond. The damage is initiated after the normal or the shear failure stresses is reached and grows linearly with increasing crack distance. The contact totally fails after the crack opening exceeds a critical value, defined by the energy release rate, and is replaced by a classical surface to surface contact [8]. The frame was meshed with an element length of 4 mm.

4.2. Modelling strategy

In contrast to more classical composites, the fibre architecture of braided composites is strongly influenced by the manufacturing process. Axial yarn content and yarn ondulation are two of the most important parameters which have to be taken into account when simulating braided structures. The axial yarn volume content mainly depends on the braiding angle and decreases by increasing the braiding angle, from 30% for 30°-braids to 20% for 60°-braids. Due to yarn waviness, braided composites show a reduced stiffness and strength in tension and compression compared to unidirectional composites. Since the tow ondulation cannot be measured with precision, reductions of 10% and 20% of the standing yarns properties and braiding yarns properties respectively have been assumed for the structure simulations. The pristine material properties of the yarns were determined by applying Chamis' theory (with a fibre content of 60%) to the constituent properties (carbon fibres and epoxy resin) [9]. Using the material model MAT_058 and reduced material properties for the yarns, the behaviour of braided composites under multiaxial loading was simulated.

4.3. Results and discussion

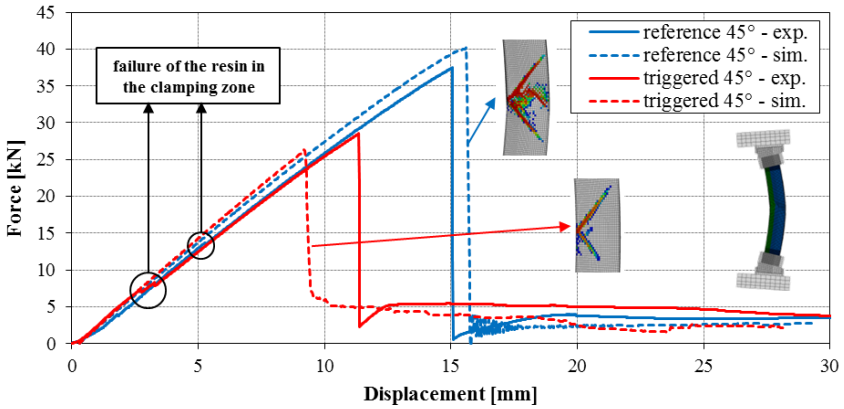

Figure 13. Simulation results for the reference and the triggered frames in comparison to the experimental results, highlighted is the crack propagation in the frame

The numerical simulations for the reference 45°-braided frame and the triggered 45°-braided frame are in relative good agreement compared to the experimental tests, as it is shown in Figure 13. In the reference simulation, the frame possesses almost the same stiffness as in the test and fails at a load of 40 kN (+5.8% in comparison to the test). The post-failure energy absorption occurs at an average force of 2 kN (experimental 3.5 kN). Due to failure of the resin in the clamping zone, which wasn't observed in the simulation, the numerical result of the triggered frame deviates from the experiment with a failure load of 26 kN (experimental 28.5 kN) and a displacement at failure of 9 mm (experimental 11.4 mm). The simulated post-failure load of 5 kN correlates with the experimental load. As in the experiment, the trigger initiates the frame failure in the triaxial layers and the cracks propagate in the biaxial layers along the 45°-directions. The discrepancies result amongst other from the complexity of braided structures - especially in the trigger zone - and their locally variable axial and braiding yarn content or braiding angle, which couldn't be experimentally measured precisely.

Excerpt from ISBN 978-3-00-053387-7

5. Conclusion

In the project DLR@UniST, alternatives to metallic aircraft components have been investigated. Based on the circular braiding process, several carbon fibre reinforced frames were manufactured and tested under combined compression - bending load. One focus of this study was to investigate most promising fibre architectures of prior studies with respect to energy absorption on a more complex design level. The investigated fibre architectures did not show the promising results with significant increase of energy absorption which were observed for C-frames on the element level. A second priority of this study was the development of a trigger mechanism for Ω-frames in combination with circular braiding process. The trigger mechanism was manufactured by overbraiding of a displacer with a diameter of 10 mm which was attached on the mandrel. The Ω-frame with trigger mechanism failed at defined location. The failure load was about 24% lower compared to the untriggered Ω-frame. Using the FE-Software LS-DYNA, it was possible to recreate the response of the frames under combined loading and to simulate the behavior of braided composites. To improve the reliability of the simulation for braided composites, the real roving structure and manufacturing deffects must be taken into account. Detailed investigations must be still performed to better understand the complexity of braided composites, especially their post-failure behaviour.

Acknowledgments

The authors wish to thank Harald Kraft and Cedric Martin for valuable discussions and support on test activities.

Funding

The research leading to these results has received funding from the Helmholtz Association of German Research Centres. The authors gratefully acknowledge the fundung of the research activities.

References

[1] R. Sturm und F. Heieck, „Energy absorption capacity of braided frames under bending loads,“ *Composite Structures, vol. 134,* pp. 957-965, 2015.

[2] I. Kumakura, M. Minegishi, K. Iwasaki, H. Shoji, H. Miyaki, N. Yoshimoto, H. Sashikuma, N. Katayama, A. Isoe, T. Hayashi, T. Yamaoka and T. Akaso, “Summary of vertical drop tests of YS-11 transport fuselage section,” *SAE Paper 2003-01-3027,* 2003.

[3] M. S. Williams and R. J. Hayduk, “Vertical drop test of a transport fuselage section located forward the wing,” *NASA TM-85679,* 1983.

[4] R. Sturm, “Untersuchung der Schadensinitiierung doppelschaliger Rumpfpaneele unter crashrelevanter Druck- Biegebelastung,” *DLR-FB-2016-18,* 2014.

[5] R. Sturm, Y. Klett, C. M. Kindervater and H. Voggenreiter, “Failure of CFRP airframe sandwich panels under crash-relevant loading conditions,” *Composite Structures, vol. 112,* pp. 11-21, 2014.

[6] K. E. Jackson, R. L. Boitnott, E. L. Fasanella, L. E. Jones and K. H. Lyle, “A history of full-scale aircraft and rotorcraft testing and simulation at NASA Langley Research Center,” *Safety Research Conference, Lisbon, Portugal,* 2004.

[7] R. Sturm and F. Heieck, “Failure modelling of braided frames under bending loads,” *ICCS18 - 18th International Conference on Composite Structures,* 2015.

[8] S. Heimbs, S. Heller and P. Middendorf, “Simulation of low velocity impact on composite plates with compressive preload,” *7th German LS-DYNA Forum, Bamberg, Germany,* 2008.

[9] C. C. Chamis, “Mechanics of composite materials: past, present, and future,” *NASA TM-100793,* 1984.

Excerpt from ISBN 978-3-00-053387-7